Supplement of Atmos. Meas. Tech., 18, 717–735, 2025
https://doi.org/10.5194/amt-18-717-2025-supplement

Atmospheric Measurement Techniques
Open Access
EGU

Supplement of

Retrievals of water vapour and temperature exploiting the far-infrared: application to aircraft observations in preparation for the FORUM mission

Sanjeevani Panditharatne et al.

Correspondence to: Sanjeevani Panditharatne (s.panditharatne21@imperial.ac.uk)

S1 Additional Covariance Matrices

Figure S1 shows the a-priori covariance for surface emissivity that was developed for the FSI extension of the Infrared Microwave Sounding retrieval scheme. This was calculated for land and sea surface types individually and then combined for the final covariance shown. For sea cases, the covariance of the surface emissivity was found using the IREMIS atlas for 17 April, 17 July, and 17 October 2013. For land cases, the surface emissivity produced by the IREMIS atlas is fixed in the far-infrared, and so the covariance was instead found using the Huang et al. (2016) emissivity database that covers the FSI spectral range.

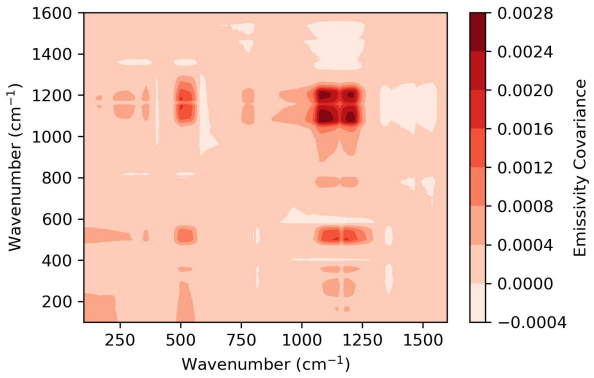

Figure S1. The a-priori covariance for the surface emissivity calculated for the FSI. This was derived from the combination of covariances of the (sea) IREMIS atlas and the (land) Huang et al. (2016) emissivity database.

Figure S2 shows the measurement covariance built for the FSI separated into contributions from the target NESR (Figure S2a) and target ARA (Figure S2b) as approximations to the noise and calibration components of the uncertainty. The covariance for the apodised NESR includes the effects of the strong Norton-Beer apodisation and has 4 sets of non-zero off-diagonals. The target ARA is specified in brightness temperature and is converted into radiance units for each individual spectrum. We assume the covariance is fully correlated. Figure S2b shows the average covariance for the ARA in radiance space calculated from the ECMWF 83 profiles as an example. Figure S2c shows the final measurement covariance, and it is the square-root diagonal of this that is shown in Figure 9b.

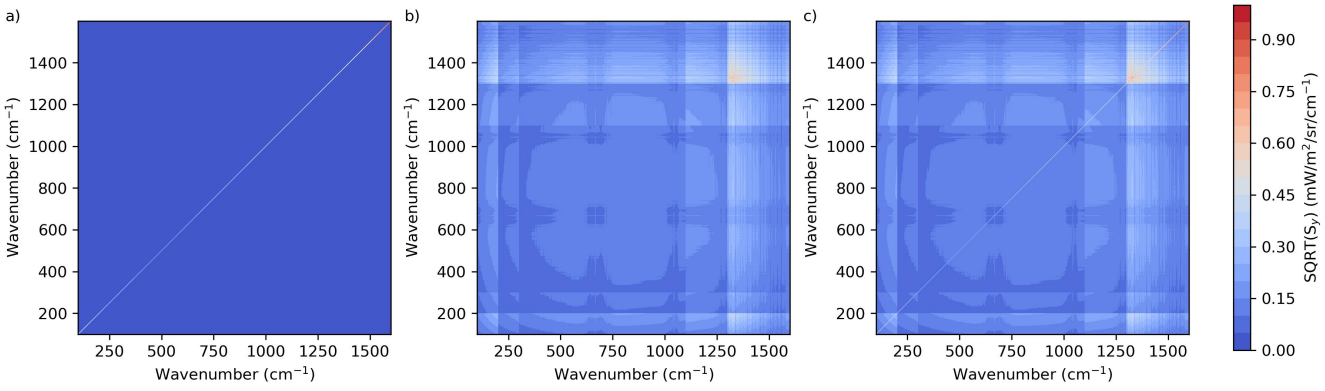

Figure S2. Components of the measurement covariance developed for the FSI. (a) Contributions from the apodised target NESR to the final measurement covariance. (b) The average contribution from the target absolute radiometric accuracy (ARA) when applied to the ECMWF 83-profiles as an example. (c) An example measurement covariance as the combination of these two components.

Following the work in Section 7.1, it was found that the a-priori covariance for temperature used in retrievals from the aircraft observations had to be tightened due to uncertainties associated with the ARIES observations. As a result, a new a-priori covariance for temperature was derived from ERA5 data for the duration of the flight surrounding the straight level runs, and this is shown in Figure S3. This is referred to as the 'local' a-priori covariance in the main text.

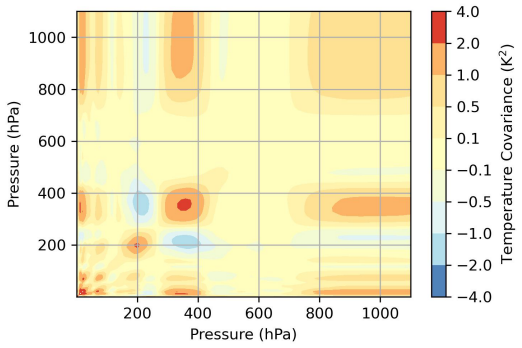

Figure S3. The local a-priori covariance for temperature used in retrievals from aircraft observations. This was calculated using ERA5 data surrounding the SLR for the duration of the flight.

S2 Retrieval Outputs from Simulations

Figure S4 shows the median water vapour and temperature bias of the retrieved profiles across the 240 testing cases for the FORUM and FORUM-aircraft configurations. The FORUM configuration outputs shown are the same as in Figure 5. As described in the main text, the biases are comparable between the two. However, the ESD associated with the FORUM-aircraft configuration is up to 15 % and 0.6 K larger for temperature and water vapour, respectively, in the mid to lower troposphere.

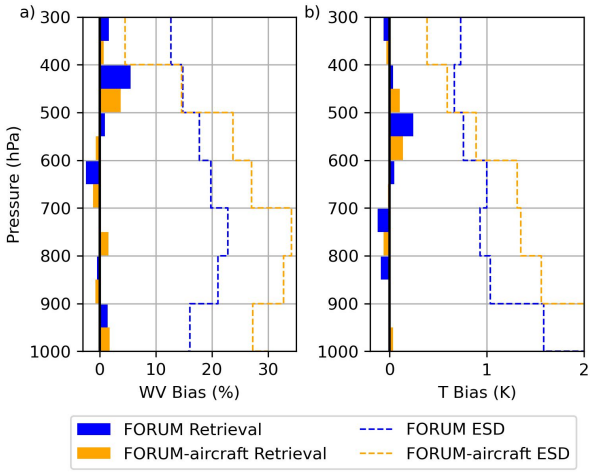

Figure S4. The median **(a)** water vapour (WV) and **(b)** temperature (T) bias of the retrieved profile to the true state across the testing cases for the optimised FORUM and FORUM-aircraft configurations in blue and orange respectively. Biases are evaluated between 300 and 1000 hPa in 100 hPa bins as in Trent et al. (2023). Dashed lines show the median estimated standard deviation (ESD) for a single retrieval for the test cases in each bin. For water vapour this is plotted with an offset of - 10% for clarity.

Figure S5 shows the median surface emissivity and skin temperature retrieved from the 240 test simulations using all three different configurations described within this paper (IASI, FORUM, and FORUM-aircraft). Figure S5a shows that in all three cases, the retrieved emissivity is within 0.01 of the 'true' value above 250 cm^{-1}. Larger median residuals are observed below 250 cm^{-1} due to a lack of sensitivity in this region to the surface emissivity. Figure S5b shows all three configurations have a similar median retrieval bias for the skin temperature of approximately -0.06 K.

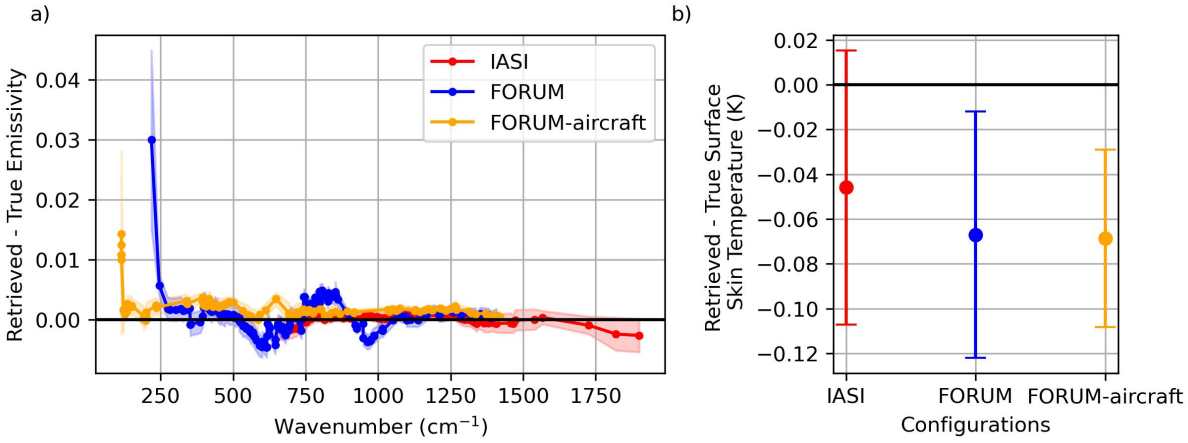

Figure S5. The median residual between the retrieved and input (a) surface emissivity and (b) surface skin temperature for the IASI (red), FORUM (blue), and FORUM-aircraft (orange) configurations across the 240 cases. The shaded regions and errorbars represent the median absolute deviation around this residual.

S3 Retrieval Outputs from Observations

Figure S6 shows the retrieved surface emissivity in each channel from each of the selected aircraft observations. Above 160 cm^{-1}, there is a considerable agreement between all of the retrievals. At lower wavenumber, the retrieved emissivity diverges due to a limited sensitivity to it in this region.

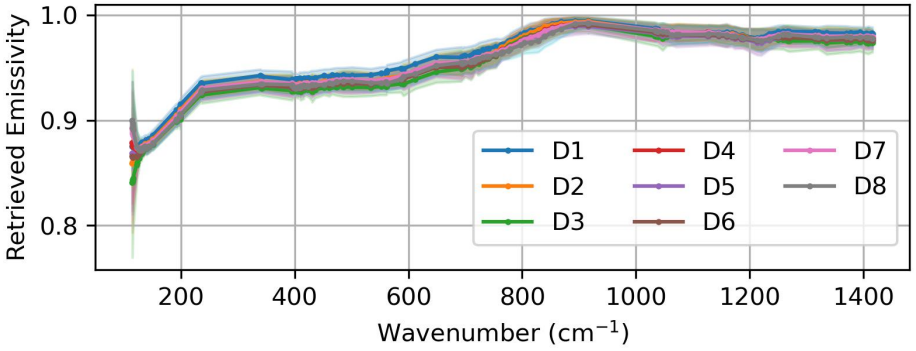

Figure S6. The retrieved surface emissivity in each channel from the aircraft observations. Shading represents one ESD.

Figure S7 shows the water vapour biases associated with the retrievals from observations in Section 7.2 in more detail for clarity. Figure S7a and b show the water vapour biases in ppmv units against each individual AK-treated dropsonde profile. Figure S7c shows this same residual but as a percentage bias.

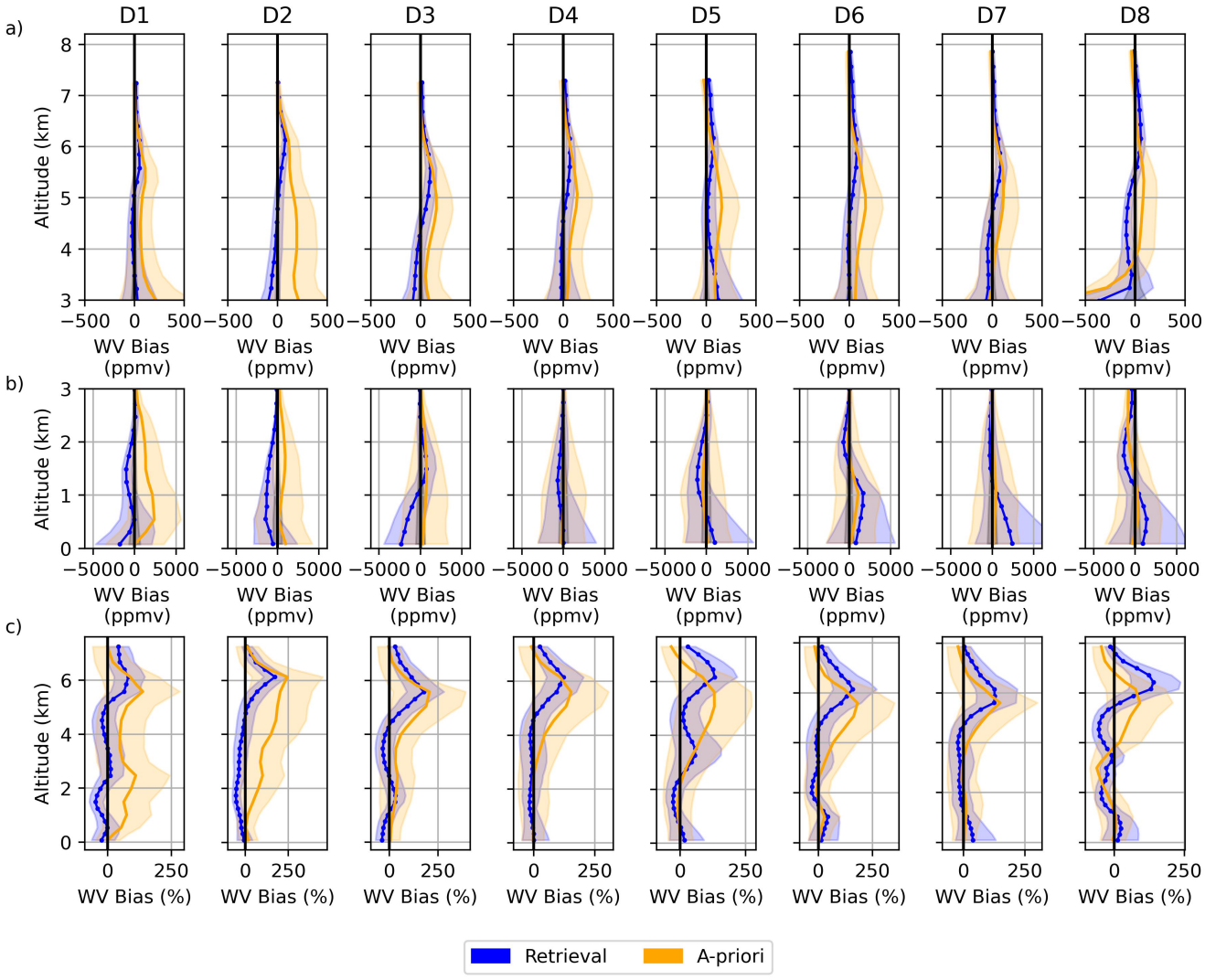

Figure S7. The difference between retrieved water vapour and AK-treated dropsonde profiles performed on the FORUM-aircraft radiances. (a,b) These are shown in ppmv and have been separated into (a) above 3km and (b) below 3 km for clarity. The percentage water vapour bias is shown in (c). The shaded region around each retrieved value represents two ESD. The a-priori is shown in orange with the shaded region showing the a-priori standard deviation. The shading around the zero line (black) represents the uncertainties outlined in Section 5.1.2. For temperature, the dropsonde uncertainty is represented as 0.2 K. For water vapour, the dropsonde uncertainty varies with altitude but remains below 9%.

References

Huang, X., Chen, X., Zhou, D. K., and Liu, X.: An observationally based global band-by-band surface emissivity dataset for climate and weather simulations, Journal of the Atmospheric Sciences, 73, 3541–3555, https://doi.org/10.1175/JAS-D-15-0355.1, 2016.

Trent, T., Siddens, R., Kerridge, B., Schroeder, M., Scott, N. A., and Remedios, J.: Evaluation of tropospheric water vapour and temperature profiles retrieved from Metop-A by the Infrared and Microwave Sounding scheme, Atmospheric Measurement Techniques, https://doi.org/10.5194/amt-16-1503-2023, 2023.